Indian Journal of Chemical Technology
Vol. 24, July 2017, pp. 435-440

Water treatment using photocatalytic and antimicrobial activities of tin oxide nanoparticles

Sunil Kumar*[,1,4], Manish Kumar[1], Alpana Thakur[2] & Sushma Patial[3]

[1]Department of Chemistry, Sri Sai University, Palampur, India

[2]Department of Physics, Himachal Pradesh University, Shimla, India

[3]Department of Chemistry, Shoolini University, Solan, India

[4]Department of Chemistry, Govt. Degree College, Khundian (Kangra), India

E-mail: sunil678kumar@rediffmail.com

Received 18 February 2016; accepted 22 July 2016

Wet chemical synthesis of nanomaterial has earned reputation for producing size and shape controlled nanomaterials with fair reproducibility. In the present work, size controlled tin oxide nanoparticles have been synthesized by chemical precipitation method using SDS as capping agent. X-ray diffraction spectra (XRD) confirm the formation of tetragonal rutile SnO_2 nanoparticles with average crystallite size in the range of 25-35 nm. Fourier Transform Infrared Spectroscopy (FTIR) complimented the XRD results with the peak of Sn-O-Sn stretching at 643 cm^{-1}. Surface morphology of prepared nanoparticles has been studied with the help of scanning electron microscopy (SEM). A direct band gap of 2.97 eV has been calculated for the synthesized nanoparticles using UV-Vis spectra and Tauc plots. Synthesized nanoparticles show excellent photocatalytic degradation of water pollutant dye congo red and also illustrate antimicrobial action against human pathogen bacteria *Pseudomonas aureginosa* and *Staphylococcus aureus*.

Keywords: SnO_2, XRD, Photocatalytic, Antimicrobial

Nanotechnology plays a major role in the development of new products with improved properties and environment friendly nature. Nanomaterials find their applications in the fields of cosmetics, textiles, paints, medicine, energy and environment[1-4].

Nanostructures of metal oxide have been explored in the recent past due to their exciting properties and applications. Nano tin oxide has been one of the most important oxide nanostructure due to their properties and potential application[5-7]. Nano tin oxide is among the most explored metal oxides as it has properties of wide band gap semiconductor. It has high optical transparency, chemical sensitivity which makes it a very attractive material for solar cells, heat mirrors, catalysis and gas-sensing applications[8]. Nanoparticles of tin oxide have also find applications in ceramic devices, lithium batteries, transparent electrodes and photocatalysts[9-12].

TiO_2, SnO_2 and ZnO have been identified as dynamic photocatalysts for the degradation of several organic contaminants including synthetic dyes[13,14]. Nano SnO_2 possesses many active sites on the surface giving rise to elevated radiations absorption efficiency and high surface reactivity thus making it suitable for photocatalyst[15]. These may be used in future at large scale water purification because SnO_2 nanoparticles show better physiochemical and catalytic properties[16]. Nano SnO_2 has been reported to possess as well as to increase antimicrobial activities[17].

There are several reported methods for the synthesis of nanomaterials including synthesis of nano tin oxide[18-25]. In the present work, SnO_2 nanoparticles were prepared by simple chemical precipitation method and have been employed for the remediation of water pollutant dyes and microbes.

Experimental Section

Materials

Dihydrated tin chloride ($SnCl_2.2H_2O$) was used as precursor and was procured from Sigma-Aldrich. Sodium dodecyl sulphate (SDS), ethylene glycol, ammonia and congo red dye ($C_{32}H_{22}N_6Na_2O_6S_2$) (Fig. 1) were supplied by S. D. Fine Chemicals. All the chemicals were of analytical grade and were used as supplied, without any further purification. Double distilled water with specific conductance in the range of 0.1×10^{-6} to $1.0\times10^{-6}\Omega^{-1}cm^{-1}$ was used for carrying out all experiments[26,27].

Synthesis of SnO_2 nanoparticles

SnO_2 nanoparticles were prepared by the use of surfactant assisted chemical route employing SDS as capping agent. Separate solutions of SDS and tin chloride were prepared and mixed at room temperature to generate a stable suspension. Ethylene glycol was added into the prepared dispersion under continuous stirring. Subsequently ammonia solution was added drop wise to keep the *p*H above 7 and mixture was stirred for two hours. The resulting solution was kept overnight and then centrifuged to

separate the solid product. Precipitates were washed several times with distilled water and ethanol. Precipitates were dried under vacuum followed by sintering at 400°C for 2 h to get fine powder of SnO_2.

Characterization

The molecular structure information of the particles was collected by FTIR spectra (Perkin-Elmer BXII FTIR spectrometer). The crystalline phase of SnO_2 particles were determined by X-ray diffraction (Panalytical S X. Pert Pro) using CuK_α radiation with a wavelength λ =1.5418 Å at 2θ values between 20° to 80°. The surface morphologies of samples were characterized using SEM (Quanta 250 FEI D9393). The dc resistivity was measured using Keithley 2611 system. UV-Vis spectra were recorded by a Systronics double beam UV-vis spectrophotometer.

Optical band gap studies

The optical band gap calculations were done by recording UV-Vis spectrum of nanomaterial suspensions prepared in ethanol by ultrasonication for 1 h. Tauc relation was then utilized to calculate band gaps using recorded UV-Vis spectrum. According to the Tauc relation [28], the absorption coefficient (α) is given by

$$ahu = B(hu - E_g)^m \quad \ldots (1)$$

where B is constant having different values for different transitions, E_g is the band gap energy, hυ is the energy of photon and m is an exponent with values 1/2, 3/2, 2 and 3 depending upon the electronic transition. The linear portion of the plot between $(\alpha h\upsilon)^2$ versus hυ taking m = 1/2 (for direct band gap semiconductors) was extrapolated to obtain the optical band gap[29].

Electrical resistivity studies

DC resistivity (ρ) of the prepared nanoparticles was obtained using I-V curves values in relation

$$P = \frac{VA}{It} \quad \ldots (2)$$

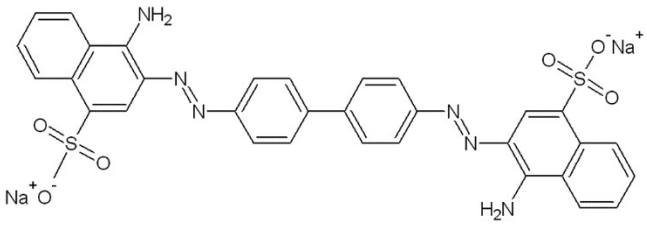

Fig. 1 — Molecular structure of congo red dye ($C_{32}H_{22}N_6Na_2O_6S_2$)

where V/I was obtained from the slope of I-V curve, A is the cross sectional area of the pellet and t is the thickness of the pellet[30]. Temperature variation of DC resistivity was also studied and the activation energy was calculated using Arrhenius equation for crystalline semiconductors

$$\sigma = \sigma_o \exp\left(\frac{E_C}{Tk_b}\right) \quad \ldots (3)$$

where, E_a is activation energy, k_b is Boltzmann constant (8.617×10^{-5} eV), T is the absolute temperature and σ_0 is the parameter depending on the material[31].

Water treatment experiments

Treatment of pollutant dyes

The water pollution due to dye congo red was treated using photocatalytic action of prepared SnO_2 nanomaterials. The effect of irradiation time on dye degradation using SnO_2 nanomaterials was studied. The experiment was done taking congo red dye (10 μmol/L) and SnO_2 nanomaterials (0.1 mg/mL) exposed to direct sunlight for recording absorbance at suitable intervals. The experiment was completed in open system nearly at 30°C and at neutral *p*H 7. The absorbance was recorded at 497 nm[32].

Treatment of bacteria

Two human pathogenic bacteria, *Pseudomonas aureginosa* and *Stphylococcus aureus* present in water were eliminated using antibacterial effect of SnO_2 nanoparticles. The method of growth curves taking optical density as an equivalent of bacterial growth was employed for the treatment of *Pseudomonas aureginosa* and *Stphylococcus aureus* bacteria. The bacteria cultures were grown in separate incubator shakers for overnight in nutrient broth (13 mg/mL). Nanomaterials (1.67 mg/mL or 3.33 mg/mL) were added subsequently to these bacterial cultures and growth of bacteria was recorded by measuring optical density at 600 nm after fixed intervals.

Results and Discussion

FTIR

The various peaks in the FTIR spectra of SnO_2 and nickel doped SnO_2 nanoparticles showed the successful synthesis of SnO_2 and nickel doped SnO_2. The peak at 643 cm^{-1} corresponds[33] to Sn-O-Sn stretching in SnO_2. Other small absorption peak at 3432 cm^{-1} is attributed to -OH groups of adsorbed

water bound at SnO_2 surface while, peak at 1018 cm^{-1} is due to C-H stretching mode. Peak at 1602 cm^{-1} is related to bending vibrations of water molecule trapped in SnO_2 sample[34].

X-ray Diffraction (XRD)

The XRD pattern of SnO_2 nanoparticles (Fig. 2) shows strong and sharp diffraction peaks suggesting perfectly crystalline nature of prepared SnO_2 nanoparticles. The various peaks at 26.5, 33.8, 37.8, 51.7, 54.7, 61.8, 65.9, 71.2 and 78.6 are well in agreement with the standard[35] SnO_2 JCPDS file no. 41-1445. The average crystallite size was found in the range of 25-35 nm and the crystal structure can be indexed as tetragonal rutile[36] with $P4_2/mnm$. The lattice constants calculated from XRD data[37-38] are a = b = 4.737 Å and c = 3.186 Å.

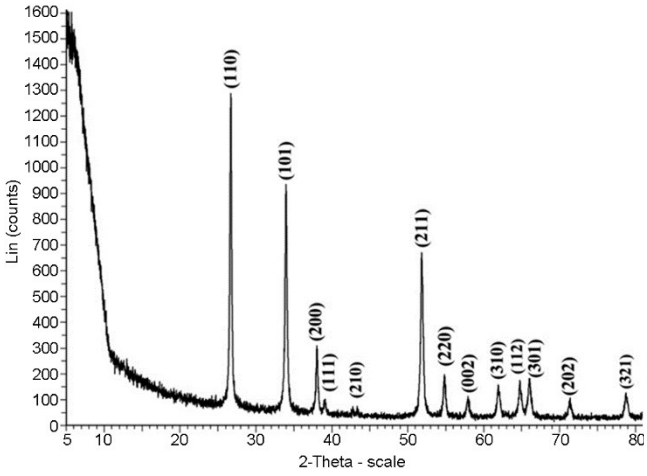

Fig. 2 — XRD pattern SnO_2 nanoparticles

Scanning Electron Microscopy (SEM)

The detailed information related to microstructure and morphology was obtained from scanning electron microscope images (Fig. 3) of prepared SnO_2 nanoparticles. Smaller individual SnO_2 nanoparticles are visible along with agglomerated SnO_2 nanoparticles at some places.

UV-Vis spectral analysis

UV-visible absorption spectra of SnO_2 nanoparticles showed absorption peak at 262 nm, which is the characteristic wavelength of tetragonal SnO_2 nanoparticles[38]. The optical band gap calculated from Tauc plots (Fig. 4) for prepared SnO_2 nanoparticles 2.97 eV which is lower than that of reported[40] SnO_2 (3.44 eV).

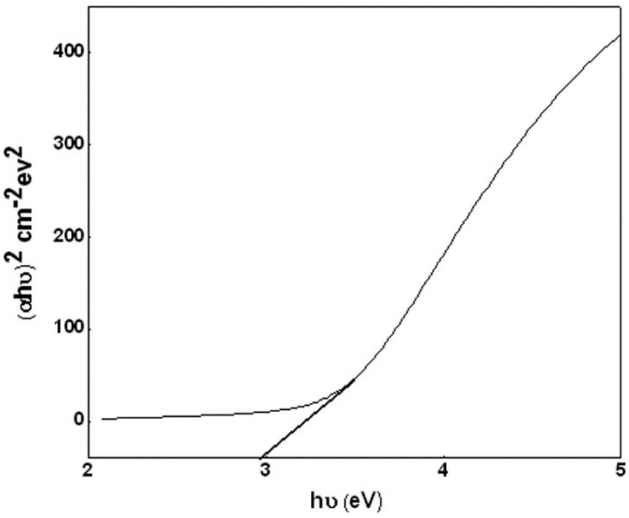

Fig. 4 — Tauc plot for SnO_2 nanoparticles

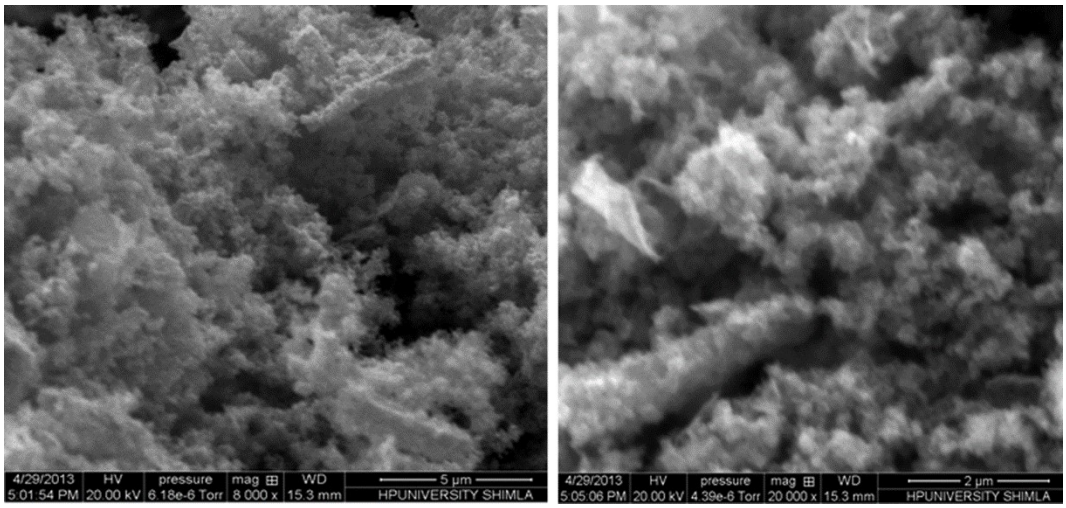

Fig. 3 — SEM images of SnO_2 nanoparticles

Electrical resistivity studies

DC resistivity of prepared nano SnO_2 was observed to be decreasing with increase in temperature (Fig. 5). This decrease in resistivity swith increase in temperature depicts the semiconducting nature of synthesized SnO_2 nanoparticles[41]. The drift mobility of the charge carriers increases with increase in temperature and participation of bound charges in the process of conduction increases thus decreasing the resistivity and increasing the conductivity[31]. The activation energy as calculated from Arrhenius equation was found to be 0.45 eV suggesting that conduction in synthesized SnO_2 nanoparticles is due to thermally supported tunneling of the charge carriers across the grain boundary and transition from the donor level to the conduction band[42].

Water treatment

Dye remediation

Photocatalytic activity of synthesized SnO_2 nanoparticles was utilized for the remediation of water polluted by congo red dye. SnO_2 nanoparticles showed high photocatalytic activity and degrade around 83% the dye in 2 h (Fig. 6).

The percent degradation of the dye was obtained using the relation

$$\%\ degradation = \left(\frac{C_0 - C_t}{C_t}\right) \times 100 \quad \ldots (4)$$

where C_0 and C_t are the dye concentrations initially and at time t respectively.

As the energy band gap of SnO_2 nanoparticles is lower than that of bulk SnO_2; on irradiation with UV-visible light, SnO_2 nanoparticles easily generate electron-hole pairs with sufficient energy to facilitate production of hydroxyl and superoxide radicals form water. These highly reactive species react abruptly with conjugated organic dye disrupting its conjugation or may also mineralize it. The photocatalytic reactions catalyzed by semiconductors involve parallel mechanisms of oxidation and reduction. Divalent Sn^{2+} ion act as electron scavenger to slow down the charge carriers' recombination and thus imparting improved photocatalytic action (Scheme 1).

The rate of photodegradation was also calculated for the degradation of congo red dye using pseudo-first-order kinetic model[43]

$$\ln\left(C_0/C_t\right) = k_a t \quad \ldots (5)$$

where k_a is the apparent rate constant. The photodegradation of congo red dye using SnO_2 nanoparticles follows the pseudo-first-order kinetics with rate constant of 0.015 min^{-1}.

Treatment of microbes

The prepared SnO_2 nanoparticles were found effective to control the growth of both *Pseudomonas aeruginosa* and *Staphylococcus aureus* bacteria (Figs 7 and 8). SnO_2 nanoparticles inhibit the growth of *Pseudomonas aeruginosa* to higher extent than *Staphylococcus aureus.* On increasing the concentration of prepared SnO_2 nanoparticles, *Pseudomonas aeruginosa* growth was more retarded whereas, *Staphylococcus aureus* growth was at less even at lower concentrations. This bacteriacidal effect may be due to binding of nanoparticles to outer membrane of bacteria causing the inhibition.

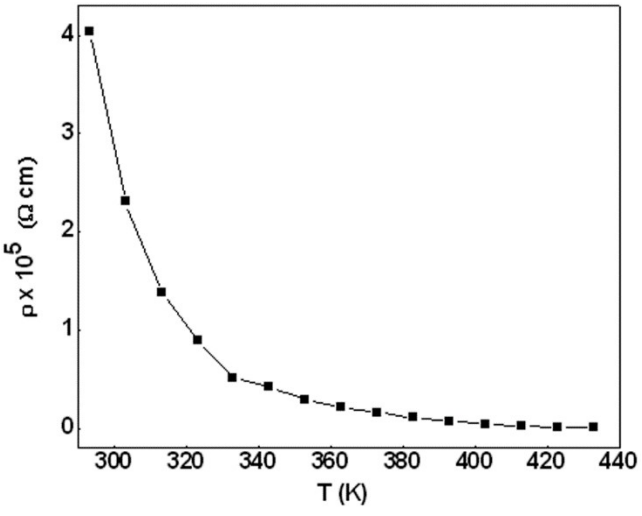

Fig. 5 — Variation of DC resistivity with temperature for SnO_2 nanoparticles

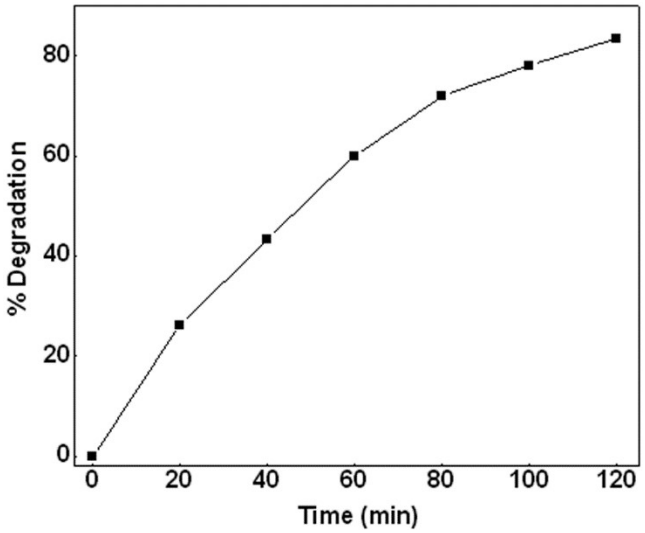

Fig. 6 — Photodegradation of congo red dye using SnO_2 nanoparticles

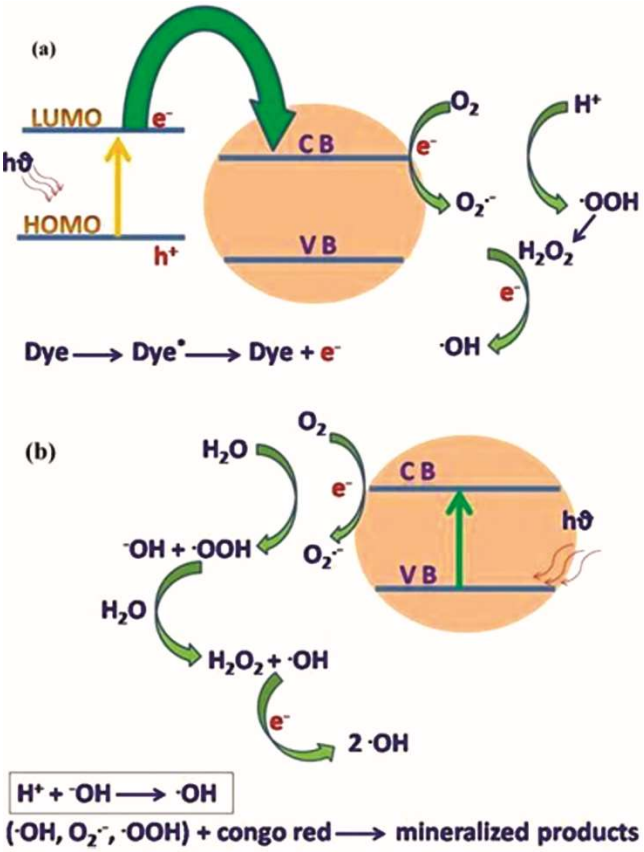

Scheme 1 — Schematic representation for photodegradation of congo red dye using SnO_2 nanoparticals under (a) visible light (b) UV light.

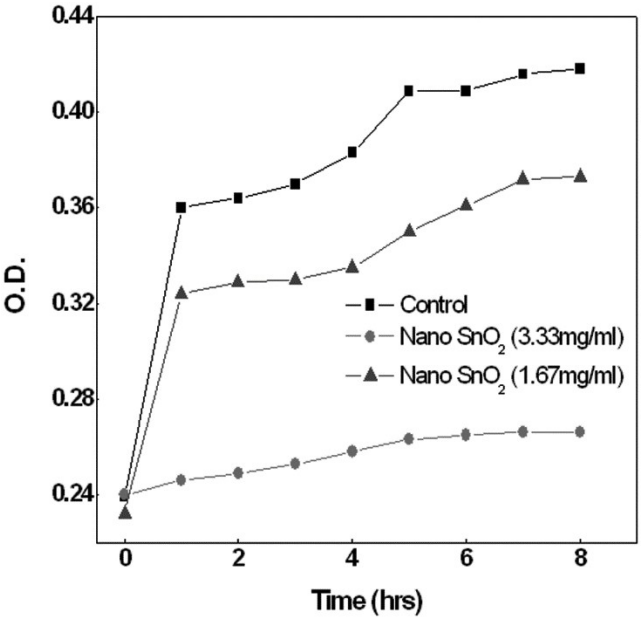

Fig. 7 — Effect of SnO_2 nanoparticles on the growth of *Pseudomonas aeruginosa* bacteria

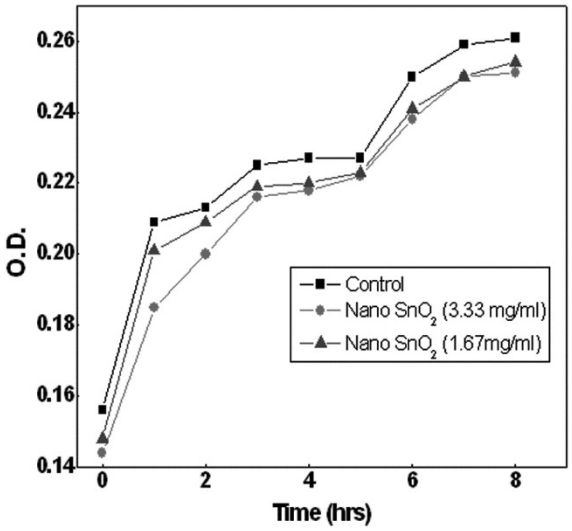

Fig. 8 — Effect of SnO_2 nanoparticles on the growth of *Staphylococcus aureus* bacteria

Conclusion

SnO_2 nanoparticles are successfully synthesized and characterized by XRD, SEM, FTIR and UV-VIS spectroscopy. XRD results reveal that synthesized nanomaterials are of crystalline nature with average crystallite size in the range of 25-35 nm. Band gap of synthesized nanoparticles is found to be 2.97 eV which enhanced the photocatalytic action of SnO_2 nanoparticles. The prepared SnO_2 nanoparticles degrade water solutions of congo red dye efficiently following pseudo-first-order kinetics. These nanoparticles also possess high bacterialcidal effect as they inhibited the growth of *Pseudomonas aeruginosa* and *Staphylococcus aureus* bacteria thus can be used in medicines.

References

1 Mackowiak S A, Schmidt A, Weiss V, Argyo C, Schirnding C, Bein T & Alexandra C B, *Nano Lett*, 13 (2013), 2576.
2 Yang Y, Zhang C & Hu Z, *Environ Sci: Processes Impacts*, 15 (2013) 39.
3 Zhang L, Pornpattananangkul D, Hu C M & Huang C M, *Curr Med Chem*, 17 (2010) 585.
4 Thakur A, Kumar S, Sharma M & Rangra V S, *Adv Mater Lett*, **7** (2016) 1029.
5 Brinker C J & Ginger D, Nanotechnology for Sustainability: Energy Conversion, Storage and Conservation: *Nanotechnology Research Directions for Societal Needs in 2020*, (Springer, Netherlands) (2011).
6 Kokura S, Handa O, Takagi T, Ishikawa T, Naito Y & Yoshikawa T, *Nanomedicine,* 6 (2010) 570.
7 Kaiser J P, Zuin S & Wick P, *Sci Tot Environ*, 442 (2013) 282.
8 Ahmeda A S, Shafeeq M, Singla M L, Tabassum S, Naqvi A H & Azam A, *J Luminescence*, 131 (2011) 1.

9 Molera J, Pradell T, Salvado N & Vendrell S M, *J Am Ceramic Soc*, 82 (1999) 2871.
10 Wu P, Du N, Zhang H, Zhai C & Yang D, *ACS Appl Mater Interf*, 3 (2011) 1946.
11 Mason T O, Gonzalez G B, Kammler D R, Mansourian H N & Ingram B J, *Thin Solid Films*, 411 (2002) 106.
12 Sangami G & Dharmaraj N, *Spectrochim Acta A*, 97 (2012) 847.
13 Kumar S, Thakur A, Rangra V S & Sharma S, *Arab J Sci Eng*, 41 (2016) 2393.
14 Hara K, Horiguchi T, Kinoshita T, Sayama K, Sugihara H & Arakawa H, *Sol Energ Mat Sol C*, 64 (2000) 115.
15 Stampfl S R, Chen Y, Dumesic J A, Niv C & Ill C H G, *J Catal*, 105, (1987) 445.
16 Dimitrov M, Tsoncheva T, Shao S & Kohn R, *Appl Catal B*, 94 (2010) 158.
17 Ayeshamariam A, Tajun M B, Jayachandran M, Kumar P G & Bououdina M, *Int J Bioass*, 2 (2013) 304.
18 Adnan R, Razana N A, Rahman I A & Farrukh M A, *J Chinese Chem Soc*, 57 (2010) 222.
19 Pinjari D V, Pandit A B & Mhaske S T, *Indian J Chem Technol*, 23 (2016) 221.
20 Chacko S, Bushiri M J & Vaidyan V K, *Mater Sci Eng B*, 96 (2006) 247.
21 Patil G E, Kajale D D, Gaikwad V B & Jain G H, *Int Nano Lett*, 2 (2012) 1.
22 Jouhannaud J, Rossignol J & Stuerga D, *J Solid State Chem*, 181 (2008) 1439.
23 Wang Y D, Ma C L, Sun X D & Li H D, *Nanotechnol*, 13 (2002) 565.
24 Cukrov L M, Tsuzuki T & McCormick P G, *Scripta Mater*, 44 (2001) 1787.
25 Hammad T M & Hejazy N K, *Int Nano Lett*, 1 (2011) 123.
26 Kant S & Kumar S, *J Chem Eng Data*, 58 (2013) 1294.
27 Kant S, Kumar A & Kumar S, *J Mol Liq*, 150 (2009) 39.
28 Seoudi R, El-Bailly AB, Eisa W, Shabaka A A, Soliman S I, Abd El R K & Romadan R A, *J Appl Sc Res*, 8 (2012) 658.
29 Sahay P P, Nath R K & Tewari S, *Cryst Res Technol*, 42 (2007) 275.
30 Shirsath S E, Toksha, B G, Mane, M L, Dhage, V N, Shengule, D R, Jadhav, K M, *Powder Technol*, 212 (2011) 218.
31 Chand J, Kumar G, Kumar P, Sharma S K, Knobel M & Singh M, *J Alloys Compds*, 509, (2011) 9638.
32 Ngieng N S, Zulkharnain A, Roslan H A & Husaini A, *ISRN Biotechnol*, 260730 (2013) 1.
33 Zhang J & Gao L, *J Solid State Chem*, 177 (2004) 1425.
34 Bharti B, Kalia S, Kumar S, Kumar A & Mittal H, *Int J Polym Anal Charact*, 18, (2013) 596.
35 Zhu J, Lu Z, Aruna S T, Aurbach D & Gedanken A, *Chem Mater*, 12 (2000) 2557.
36 Lim H N, Nurzulaikha R, Harrison I, Lim S S, Tan W T, Yeo M C, Yarmo M A & Huang N M, *Ceramics Int*, 38 (2012) 4209.
37 Pouretedal H R, Shafeie A & Keshavarz M H, *J Korean Chem Soc*, 569 (2012) 484.
38 Baur, W H *Acta Cryst*, 9 (1956) 515.
39 Chen W, Ghosh D & Chen S, *J Mater Sci*, 43 (2008) 5291.
40 Benhebal H & Chaib M, *African J Basic ApplSci*, 3 (2011) 228.
41 Han J, Mantas P Q & Senos AMR, *J Eur Ceram Soc*, 21 (2001) 1883.
42 Patidar D, Rathore K S, Saxena N S, Sharma Kananbala & Sharma T P, *Chalcogenide Letters*, 5 (2008) 21.
43 Malian E P, Diaz O G, Arana J, Rodriguez J M D, Rendon E T & Melian J A H, *Catal Today*, 129 (2007) 256.